◆ Human Brain Mapping 38:1952–1964 (2017) ◆

The Human Subthalamic Nucleus and Globus Pallidus Internus Differentially Encode Reward during Action Control

Peter Justin Rossi,[1]* Corinna Peden,[2] Oscar Castellanos,[2] Kelly D. Foote,[1] Aysegul Gunduz,[2] and Michael S. Okun[1]

[1]*Center for Movement Disorders and Neurorestoration, University of Florida, Gainesville, Florida*
[2]*J. Crayton Pruitt Family Department of Biomedical Engineering, University of Florida, Gainesville, Florida*

Abstract: The subthalamic nucleus (STN) and globus pallidus internus (GPi) have recently been shown to encode reward, but few studies have been performed in humans. We investigated STN and GPi encoding of reward and loss (i.e., valence) in humans with Parkinson's disease. To test the hypothesis that STN and GPi neurons would change their firing rate in response to reward- and loss-related stimuli, we recorded the activity of individual neurons while participants performed a behavioral task. In the task, action choices were associated with potential rewarding, punitive, or neutral outcomes. We found that STN and GPi neurons encode valence-related information during action control, but the proportion of valence-responsive neurons was greater in the STN compared to the GPi. In the STN, reward-related stimuli mobilized a greater proportion of neurons than loss-related stimuli. We also found surprising limbic overlap with the sensorimotor regions in both the STN and GPi, and this overlap was greater than has been previously reported. These findings may help to explain alterations in limbic function that have been observed following deep brain stimulation therapy of the STN and GPi. *Hum Brain Mapp 38:1952–1964, 2017.* © 2017 Wiley Periodicals, Inc.

Key words: deep brain stimulation; basal ganglia; parkinson's disease; reward; subthalamic nucleus; globus pallidus

INTRODUCTION

The study of subcortical involvement in the reward system has largely focused on the striatum, the nucleus accumbens, and the ventral pallidum [Breysse et al., 2015]. Roles for the subthalamic nucleus (STN) and the globus pallidus internus (GPi) in reward circuitry have only recently been recognized [Hikosaka et al., 2008]. High frequency stimulation of the STN and GPi has been associated with limbic system pathologies in humans with Parkinson's disease, including depression, suicidal ideation, apathy, mania, and impulsivity [Rossi et al., 2015]; improvements in limbic symptoms, such as relief of obsessive compulsive symptoms [Nair et al., 2014], self-mutilation behavior [Cif et al., 2007], and addiction [Witjas et al., 2005] have also been reported. Understanding the neurobiological substrates of human STN and GPi involvement in reward circuitry may help explain chronic stimulation-related alterations in limbic function.

Aysegul Gunduz and Michael S. Okun are co-senior authors on this manuscript.
*Correspondence to: P. Justin Rossi, 3450 Hull Road, Gainesville, FL. E-mail: pjrossi@ufl.edu

Received for publication 7 October 2016; Revised 20 November 2016; Accepted 7 December 2016.
DOI: 10.1002/hbm.23496
Published online 28 January 2017 in Wiley Online Library (wileyonlinelibrary.com).

Substantial evidence from animal studies over the past decade indicates that the STN plays an important role in processing reward [Rossi et al., 2015]. Large subsets of STN neurons in the rat have been shown to encode the prospect of reward, reward receipt, and the magnitude of possible reward outcomes. Similar responsiveness to reward has been demonstrated in non-human primates [Darbaky et al., 2005; Espinosa-Parrilla et al., 2013, 2015].

Studies in non-human primates suggest that the GPi also has a role in reward processing [Hikosaka et al., 2008]. Certain GPi neurons in the monkey project to the lateral habenula (LHb), a known limbic structure, and these neurons appear to encode reward prediction [Hong and Hikosaka, 2013; Matsumoto and Hikosaka, 2007]. A study of individual neuron behavior in monkeys performing reward-motivated limb movements identified a population of GPi neurons that modulated firing rate in response to reward delivery [Gdowski et al., 2007]. These findings have recently been corroborated in humans. Howell et al. identified GPi neurons in Parkinson's patients that modulate their firing rate significantly in response to reward-related stimuli

[Howell et al., 2016]. Local field potential recordings from the GPi in humans showed correlation between pallidal LFP amplitude and reward expectation [Schroll et al., 2015]. Finally, functional neuroimaging has shown greater neural activation in the human pallidum in response to rewards as compared to response to neutral stimuli [Bischoff-Grethe et al., 2015].

The construct of "reward" falls under the broader construct of *valence*, defined as the intrinsic attractiveness or aversiveness of a stimulus. Rewarding stimuli are considered positively valenced while aversive stimuli are considered negatively valenced [Lane et al., 1999]. Valence and action control are intimately intertwined in that organisms tend to act or inhibit action to obtain positively valenced outcomes and to avoid negatively valenced outcomes. Elucidating the neurobiological bases for these interactions could have implications for treating certain neuropsychiatric disorders, such as impulsivity, where valence perception and action control mechanisms are considered dysfunctional [Rossi et al., 2015].

The present study aimed to establish if (and how) human STN and GPi neurons encode valence information during action control. We assessed the behavior of individual neurons in the STN or GPi of human Parkinson's disease patients while they performed a task in which action choices were associated with rewarding, punishing, or neutral outcomes. Briefly, participants learned to associate a visual stimulus (one of four color patches) with one of four action-valence combinations: a reward for action, a punishment for action, a reward for withholding action, and a punishment for withholding action (Fig. 1). Thus, in each trial, participants were motivated by the desire either to obtain a reward or avoid punishment. Rewards and punishments were a monetary gain or loss, respectively, and action involved pressing of a button on a joystick with the hand contralateral to the brain region being recorded. Neuronal responsiveness was assessed by comparing the activity during an inter-trial interval with that of the post-stimulus period (see methods). We assessed for changes in firing rate following the presentation of stimuli signifying the need to make a response and stimuli giving feedback. We analyzed neuronal data only for iterations of the task where patients made the optimal response in greater than 60% of trials, to ensure that participants had learned the intended action-valence association.

Our working hypothesis was that both STN and GPi neurons would modulate activity in response to predictors of positively and negatively valenced outcomes (opportunity for reward and threat of punishment) and attained valence outcomes (reward receipt and loss avoidance). Our results revealed that STN and GPi both encoded valence-related information but that the proportion of valence-responsive neurons was significantly greater in the STN. Among STN neurons, reward mobilized a greater proportion of neurons than did loss avoidance. These findings may provide at least part of a neurobiological basis for the altered limbic function that has been observed following electrical stimulation of the STN and GPi in humans.

MATERIALS AND METHODS

Patients

Patients with Parkinson's disease undergoing unilateral de novo STN or GPi deep brain stimulation (DBS) electrode placement surgery were studied. All patients fulfilled the UK Brain Bank diagnostic criteria for PD [Daniel and Lees, 1993]. All participants were non-demented. A total of 53 patients participated and had a mean age of 65.7 years (STD = 7.85). The Institutional Review Board approved the study and all patients provided informed consent before enrollment.

Behavioral Task

The behavioral task used in the study was based on the design pioneered by Guitart-Masip et al. [Guitart-Masip et al., 2012a,b] and modified by van Wouwe et al. [van Wouwe et al., 2015]. All stimuli were presented on a 15-inch screen positioned at eye level approximately one meter from the patient. Responses were made with the thumb contralateral to the brain hemisphere recorded using a handheld, single-button joystick. In the preoperative clinic approximately 24 h prior to surgery, subjects completed practice sessions (two blocks) of the action-valence learning task to associate combinations of action (action, inaction) and valence (reward acquisition, loss avoidance) to a specific stimulus color. The same action-valence learning task was then presented to the subject

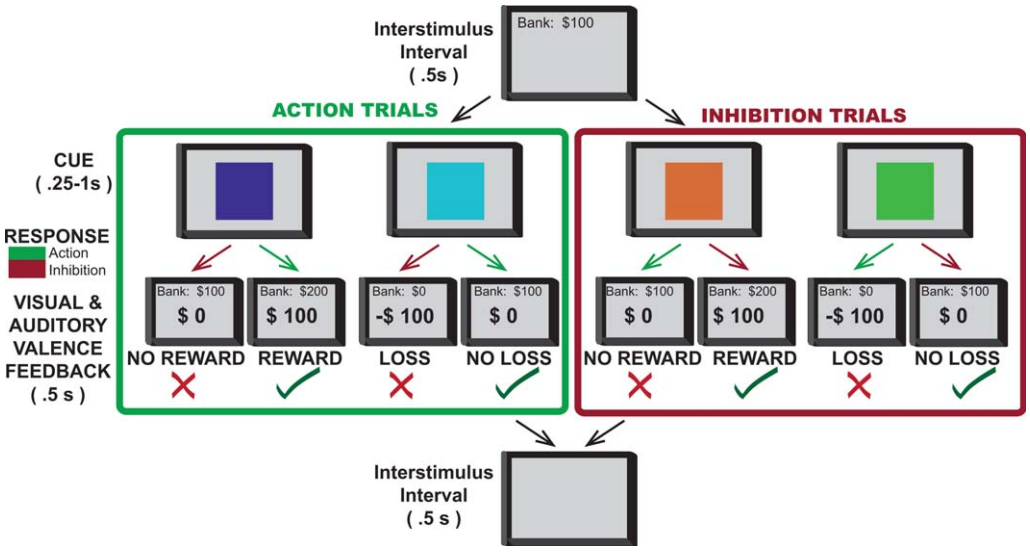

Figure 1.

Valence-Action Task. On each trial, one of four possible color patches indicated the combination of required action (making or withholding button press) and outcome valence (win, loss, or no gain). An action decision was required following presentation of the color patch. After a brief delay, the outcome was presented: "+$100" in green indicated a reward, a red "−$100" indicated a loss, and a black "$0" indicated the absence of a win or a loss. In go to win trials (purple cue), button press was rewarded; in go to avoid losing trials (blue cue), button press avoided punishment; in no-go to win trials (orange cue) withholding button press was rewarded, and in no-go to avoid losing trials (green cue) withholding button press avoided punishment. A running total score was presented at the top of the screen throughout the task. Each trial was preceded by an interstimulus interval in which a blank screen was presented. Stimuli were presented in pseudorandom order for a total of 120 trials (30 trials of each color/condition).

intraoperatively during the microelectrode-recording (MER) phase of the DBS operation.

The details of the action-valence task are as follows (Fig. 1). Upon the presentation of a color patch, subjects were instructed that they had 1,000 milliseconds (ms) to either act (i.e., make a button press) or to withhold action. Button press or expiration of the 1,000 ms window was followed by a 250 ms delay period to facilitate separation of movement and feedback neuronal signals. Because delayed outcome of a choice is known to reduce the subjective value of the reward, the shortest possible delay duration was chosen while still permitting accurate signal separation. After this delay, feedback was displayed for 500 ms in the center of the color patch indicating that the action decision had led to monetary reward (+$100), monetary loss (-$100), or no monetary outcome ($0). Monetary rewards were accompanied by a "positive contingency" audio feedback simulating the jingle of coins. Monetary losses were accompanied by a "negative contingency" audio feedback simulating an aversive buzzer sound. The feedback and color patch were then extinguished, and an intertrial interval followed for 500 ms after which the next trial began. A running total of earnings were presented in the upper center of the screen throughout the task. The four color patches appeared in pseudorandom order and with equal probability across the 120 trials per block. Thus, each color appeared 30 times within a block of trials. Unbeknownst to the subject, two of the color patches provided outcomes that were either rewarded (+$100) or unrewarded ($0), and the remaining two colors provided outcomes that were either punished (−$100) or unpunished ($0). Thus, the former colors were associated with reward learning, whereas the latter colors were associated with loss avoidance learning. Also unknown to the subject, one color from each set produced the optimal outcome (either gain of reward or avoidance of loss) by acting, but the other color from each set produced the optimal outcome by withholding action. This design completed the 2 × 2 factor design that orthogonalized both valence and action.

Localization of Recording Sites

A proprietary stereotaxic surgical software system was used to visualize MRI images, estimate anatomical locations of the STN and GPi, define target location, predict trajectories for microelectrode penetrations, and map results of microelectrode recordings [Sudhyadhom et al., 2012]. To avoid sampling bias, cells were selected strictly on the basis of signal integrity rather than the presence or absence of sensorimotor activity [Sarma et al., 2012]. Anti-

Parkinsonian medications were withheld 24 h before neural recording, and no sedatives were given prior to or during recordings [Sarma et al., 2012].

Data Acquisition

Extracellular spiking activity of subthalamic and pallidal neurons was recorded using platinum/iridium-tipped microelectrodes (FHC, Bowdoin, ME) with impedances of 0.5–1 MΩ mounted in a motorized, hydraulic microdrive (FHC, Bowdoin, ME). The behavioral task was administered by a Dell Optiplex 9020 computer using BCI2000 software [Schalk et al., 2004]. Neuronal activity was bandpass filtered between 300 Hz–6 kHz and sampled at 48 KHz (16 bit resolution; Tucker Davis Technologies, Alachua, FL). The neuronal recording was monitored via computer display and audio speakers.

Recording Protocol

All recordings were performed using an array of three microelectrodes, separated by 2 mm in an L-shaped configuration, lowered transdurally into the STN or GPi. For recordings of the STN, the microelectrode array was configured with a central contact, a second contact positioned 2 mm laterally, and a third positioned 2 mm anteriorly. For recordings of the GPi, the microelectrode array was configured with a central contact, a second contact positioned 2 mm laterally, and a third positioned 2 mm posteriorly. Electrophysiological determination of STN and GPi borders was based on electrode depth along the planned trajectory, spontaneous firing rate and pattern, and kinesthetic responses [Toleikis et al., 2012]. When one or, less frequently, two neuronal units were isolated by at least two of the recording electrodes in the array and the recording was determined to be stable, the cognitive task was initiated. Neuronal data, electrode location, and task performance data were then collected following a standard protocol of 120 stimulus presentations (30 of each of the four conditions) in pseudorandom order to ensure an equal number of trials of each condition. Data collection was stopped only if signal quality deteriorated. Upon completion of the task, the microelectrode was advanced so that other units could be evaluated until the microelectrode array was determined to no longer be in the region of interest.

Electrophysiological Data Analysis

Amplitude thresholds for neural spike data were selected, and candidate action potentials were sorted into clusters in principal components space (Spike2, Cambridge Electronic Design, Cambridge, UK). Neurons were considered acceptable for further analysis only if their action potentials were of a consistent shape, had a clear refractory period of at least 2 ms, and could be reliably distinguished from the waveforms of other units and from background noise [Zimnik et al., 2015]. Additionally, analyzed neurons had to be associated with a complete set of task-related data (i.e., 120 stimuli trials). Peri-event time histograms (PETHs) were then constructed from the correct trials of each of the four conditions, and for the additional conditions where "incorrect" responses occurred.

Stimulus-related changes, movement-related changes, and outcome-related changes in firing rate were defined as a significant deviation from the baseline inter-trial interval. Baseline activity was defined as activity occurring in the 500 ms period that preceded cue presentation in each trial. Event-related activity was determined in the 500 ms that followed the onset of the visual stimulus (stimulus related), the 500 ms centered on the button press (movement related), the 500 ms centered on trial expiration (inhibition related), and the 500 ms that followed feedback delivery (outcome related).

Analyses were based on binned peri-event firing rates (50 ms bins). For each event of the task, we generated a PETH centered on that event using MATLAB (Mathworks, Cambridge, MA) [Lardeux et al., 2009]. For all trial types, the neuronal responses to stimulus presentation, button press, trial expiration, and feedback delivery were analyzed separately. The responses to the stimulus presentation, button press, and feedback were analyzed separately for correct and incorrect trials.

To minimize the contamination of signals by activity related to a previous event, the neural response to each event was analyzed across the 500 ms event-based epoch and was compared with the activity over the 500 ms intertrial interval preceding the onset of that trial. The 500 ms baseline interval was chosen to maximize sampling while also preventing event-related activity from colliding using the period between two consecutive events (the feedback delivery from a prior trial and the presentation the stimulus in the subsequent trial).

Analyses were performed according to the analysis of Teagarden and Rebec [2007] and Breysse et al. [2015]. Briefly, the mean firing rate for each peri-event bin was expressed as a z-score (z_i) based on the following formula: $z_i = \frac{Fq_i - \mu_{baseline}}{SEM_{baseline}}$, with Fq_i as the mean firing rate (in hertz) of the bin (i) and $\mu_{baseline}$ the mean firing rate of the intertrial baseline period preceding each event, and $SEM_{baseline}$ indicating the standard error of the mean of the baseline. Three or more consecutive bins ($\geq$150 ms) with z-scores $\geq$1.64 (95% confidence interval) were considered to be significant activation or inhibition.

Finally, for each event, neurons were classified as either "similar" or "specific" [Lardeux et al., 2009]. The firing rate of neurons that responded to an event was compared for each outcome with a t-test on the normalized data. Thus, neurons were similar if they responded to one event in a similar manner for both rewards (t-test, $P > 0.05$) [Lardeux et al., 2009]. Neurons were specific if they responded to one event for both rewards with a significantly higher

response to one reward than the other or if they responded exclusively to one outcome [Lardeux et al., 2009].

The proportions of neuronal subpopulations (e.g., "Go/Reward selective" vs. "Go/Loss selective") expressed in percentages were compared using a χ^2-test. The average of the *z*-scores of the population PETH were illustrated by separating the specificity of neurons for either each reward or correct versus incorrect trials, based on the criteria defined above (three consecutive bins with *z*-scores $\geq$1.64). The neurons were also analyzed based on their response type (activation or inhibition), and the *z*-scores have been calculated. The percentage of variation for activated and inhibited neuronal populations was calculated by comparing the mean firing rate during baseline period and during the event-related period.

Recording Site Mapping

The spatial locations of the recording sites in STN and GPi were defined in relation to the structure's borders in each individual patient utilizing proprietary surgical planning software. This software superimposes a three-dimensional, digitized version of the Schaltenbrand atlas onto the patient's preoperative MRI scan and intraoperative imaging [Sudhyadhom et al., 2012]. The atlas is deformable to improve the fit of the atlas to the subcortical anatomy of the individual patient. Determination of the borders of targeted structures was further refined by the results of intraoperative recording, and the atlas transformed accordingly. It is important to note that the digital atlas is deformable in terms of overall size and position of structures relative to the AC-PC line. In order to better visualize these positions in a two dimensional format, we then transposed the positions onto the appropriate anatomical slices of the Schaltenbrand and Bailey atlas [Schaltenbrand and Bailey, 1959] via a method previously described by Plaha and colleagues. [Plaha et al., 2006] Briefly, this method involved defining the recording position's intra-structural vertical location by measuring its distance from the structure's dorsal boundary. Anterior–posterior and medial-lateral positions were defined as a proportion of the lengths of the structure along the appropriate axis, and this spatial location was transposed onto the Schaltenbrand and Bailey atlas by proportional measurements [Plaha et al., 2006]. Finally, anatomical coordinates were derived for each recording position. These coordinates reflect the relative location of the recording site within the coordinate system of the Schaltenbrand atlas.

RESULTS

We recorded 100 STN cells from 20 patients and 100 GPi cells from 30 patients that met pre-defined signal quality criteria. The mean duration of recordings for these neurons was 224s (range: 204s–232s). STN neurons exhibited an average firing rate of 36 ± 22 Hz (mean $\pm$ SD), similar to results of other studies [Bejjani et al., 2000; Hutchison et al., 1998; Sterio et al., 2002]; the mean frequency of GPi neurons was 66.2 ± 3.4 Hz (mean $\pm$ SE), similar to the mean human GPi neuron frequency reported elsewhere [Lee et al., 2007; Levy et al., 2001].

Valence Encoding Neurons Are More Common in STN Compared to GPi

The proportions of unique neurons responding to any valence-related stimulus (opportunity for reward, threat of loss, reward receipt, or successful avoidance of loss) in the STN and GPi were compared. Overall responsiveness to valence was found to be significantly greater in the STN compared to the GPi (70% of neurons vs. 46% of neurons, $P < 0.001$, Fisher's exact test; Fig. 2).

The STN Differentially Encoded Reward Opportunity and Threat of Loss

Of the STN neurons recorded, 57% (57/100) responded to stimulus presentation. The proportion of neurons responding to reward opportunity was significantly greater than the proportion responding to the threat of loss for both the Go (38% vs. 25%, $\chi^2 = 3.916$, $P = 0.0478$, Fig. 3e) and No Go conditions (25% vs. 12%, $\chi^2 = 5.604$, $P = 0.0179$, Fig. 3f). These results highlight that STN activity was more responsive to a potential reward than a potential loss, and that this reward sensitivity occurred independent of the action context in which the stimulus was presented.

The STN Differentially Encoded Reward and Avoidance of Loss

We observed that 66% of STN neurons recorded (66/100) responded to feedback presentation during correct trials. The proportion of neurons responding to obtained reward was significantly greater than the proportion responding to loss avoidance for both the Go (48% vs. 32%, $\chi^2 = 5.33$, $P = 0.02$, Fig. 3g) and No Go conditions (27% vs. 15%, $\chi^2 = 4.34$, $P = 0.03$, Fig. 3h). These results highlight that STN activity was more responsive to reward than an avoided loss, and that this reward sensitivity occurred independent of the action context in which the stimulus was presented.

Distinct Populations of STN Neurons Encode Reward and Loss Stimuli

The majority of STN neurons that responded to stimulus presentation were valence specific (i.e., they responded exclusively to either reward opportunity or threat of loss). The degree of specificity was independent of the action condition. For example, we observed that 81.5% were

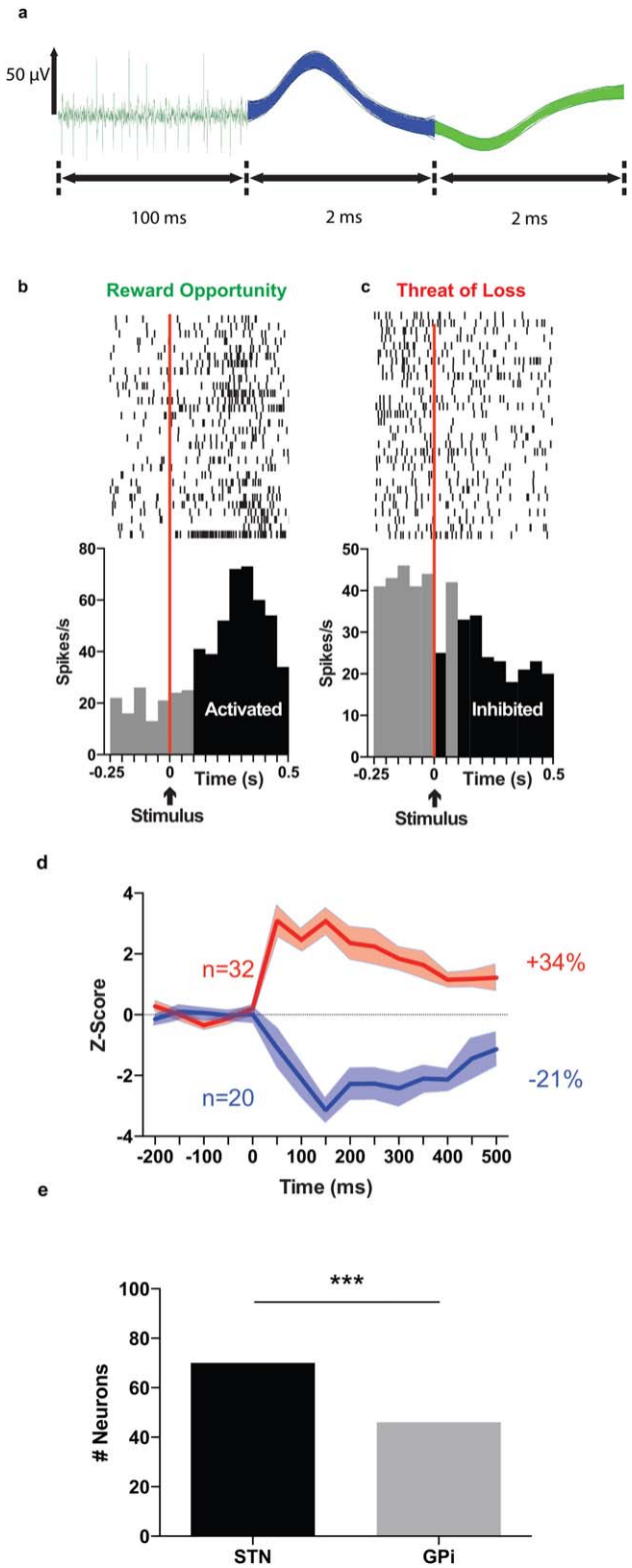

Figure 2.

specific during the Go condition and 79.1% were specific during the No Go condition. A majority of feedback responsive neurons were also valence specific (69.2% for the Go condition, 90.6% for No Go condition), and the ratios were similar to those observed following stimulus presentation. A breakdown of the relative proportions of neuron specificity is shown in Figure 3.

The GPi Similarly Encoded Reward Opportunity and Threat of Loss

We observed that 46% of GPi neurons recorded (46/100) responded to stimulus presentation. In contrast to the STN, the proportion of GPi neurons responding to reward opportunity was similar to the proportion responding to the threat of loss for both the Go (18% (18/100) vs. 14%,

Figure 2. Characterization of neuronal activity from action potentials to cell populations. **(a)** Example of different waveforms of some representative neurons recorded in the STN showing spikes (left) and biphasic waveforms (middle and right) from two distinct neurons recorded simultaneously from the same electrode. (**b)** Example of the firing pattern of one STN neuron classified as reward opportunity specific, showing increased activity in response to the color patch stimulus signifying Go for Reward. (**c)** Example of the firing rate pattern of another STN neuron classified as threat of loss specific, showing decreased activity in response to the color patch stimulus signifying Go to Avoid Loss. Rasters are centered on the occurrence of the stimulus presentation (time = 0). The stimulus is indicated with a black arrow. The area to the left of the vertical red lines represents the final 250 ms of the 500 ms baseline period (intertrial interval) on which the bins were analyzed [−500 ms: 0 ms]. The black bins represent the bins significantly different from the baseline ([0:500 ms]), with a Z-score >1.64. Light gray bins represent the bins not significantly different from baseline, with a Z score <1.64. This neuron was determined to respond with significant neuronal activation due to the occurrence of three or more consecutive bins with Z scores >1.64. Top, raster plot of spike firing on each trial (each row illustrates one trial), with the bottom row of dots corresponding to the first trial. Bottom, peri-event time histogram showing mean firing rate across all trials, with a bin size of 50 ms. (**d)** Aggregate excitation and inhibition activity of all responsive STN neurons after presentation with the stimulus signifying Go for Reward. Average z-scores (mean ± SEM) of the firing activity for all STN neurons responding by an activation (red line) or an inhibition (blue line) to the visual stimulus (time= 0 ms) in Go for Reward condition. The total number of neurons responding by excitation (red), and total number of neurons responding by inhibition (blue) are given with *n*. The percentages represent the mean variation of activity after each event for activated (red) and inhibited (blue) neuronal population. (**e**) Comparison of all unique neurons in the STN and GPi that responded to any of the valence stimuli (reward opportunity, threat of loss, reward obtained, or loss avoided). *** indicates *P* value < 0.001.

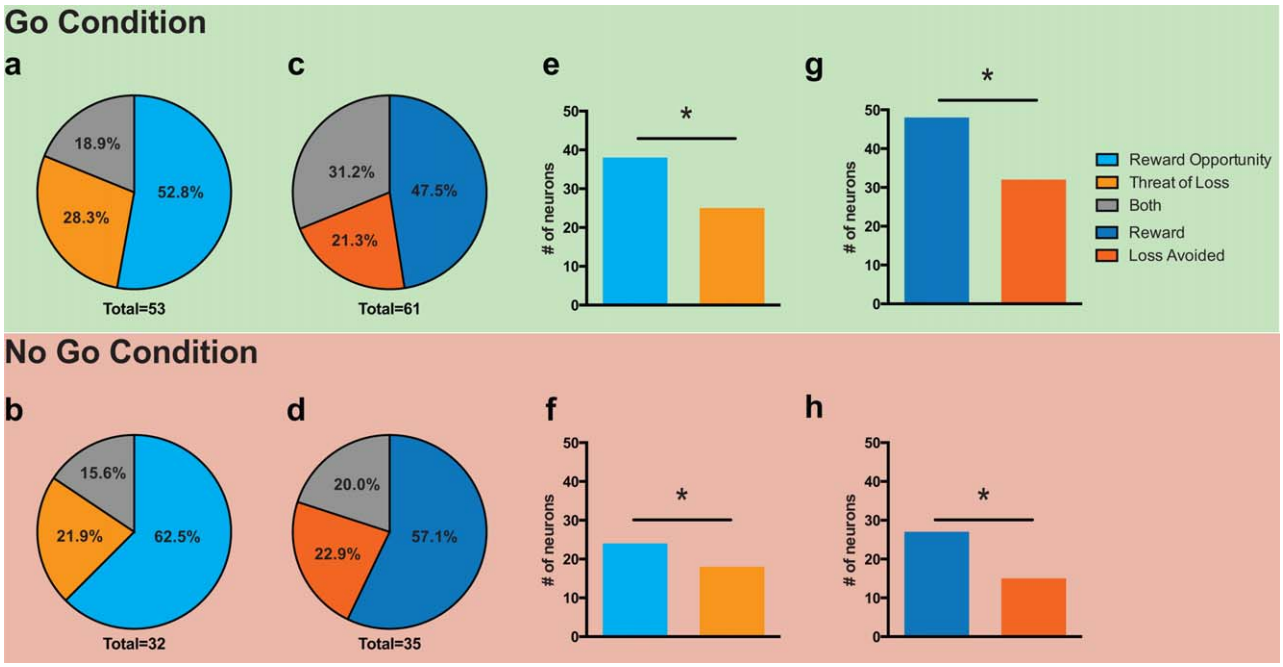

Figure 3.

STN responsiveness to valence in stimulus and feedback conditions. Proportions of the neuronal population responding in the poststimulus period to reward opportunity, threat of loss, and both conditions during Go trials (**a**) and No Go trials (**b**). Proportions of the neuronal population responding in the postfeedback period to reward, loss avoidance, and both conditions during Go trials (**c**) and No Go trials (**d**). [reward receipt (dark blue), loss avoidance (dark orange), and both (gray)]. Total number = total number of responding neurons out of 100 neurons analyzed. Comparison of neurons responding to reward opportunity and neurons responding to threat of loss for the Go (**e**) and No Go (**f**) conditions. Comparison of neurons responding to reward obtained and loss avoided for the Go (**g**) and No Go (**h**) conditions. (* = $P < 0.05$, χ^2-test).

respectively; $\chi^2 = 0.5952$, $P = 0.4404$, Fig. 4e) and No Go conditions (13%, vs. 16%, respectively; $\chi^2 = 0.363$, $P = 0.5469$, Fig. 4f).

The GPi Similarly Encoded Reward and Avoidance of Loss

We observed that 42% of GPi neurons recorded (42/100) responded to feedback presentation during correct trials. In contrast to the STN, the proportion of GPi neurons responding to reward receipt was similar to the proportion responding to loss avoidance for both the Go (26% vs. 25% $\chi^2 = 0.0263$, $P = 0.8711$, Fig. 3g) and No Go conditions (19% vs. 16%, respectively; $\chi^2 = 0.312$, $P = 0.5766$, Fig. 3h).

Distinct Populations of GPi Neurons Encode Reward and Loss Stimuli

The majority of GPi neurons that responded to stimulus presentation were also valence specific. Similar to the STN, the degree of specificity was independent of the action condition. We observed that 81.1% were specific during the Go condition and 84.4% were specific during the No Go condition.

A majority of feedback responsive neurons were also valence specific (68.8% for the Go condition, 80% for No Go condition), and the ratios were similar to those observed following stimulus presentation. A breakdown of the relative proportions of neuron specificity is shown in Figure 4.

Valence Responsive Neurons in STN and GPi Overlap Somatosensory Regions

The mean position of the recording sites in STN were 10.69 ± 1.2 mm (mean $\pm$ SD) lateral to the AC–PC line in the mid-sagittal plane, 1.34 ± 1.39 mm posterior to the intercommissural point and 3.8 ± 1.25 mm below the AC–PC plane (Fig. 5A–C). The mean position of STN neuronal populations responsive to various valence stimuli are shown in Figure 5. These were well within the accepted bounds of the somatosensory STN [DeLong et al., 1985].

The mean position of the recording sites in GPi were 22.22 ± 1.65 mm lateral to the AC–PC line in the mid-

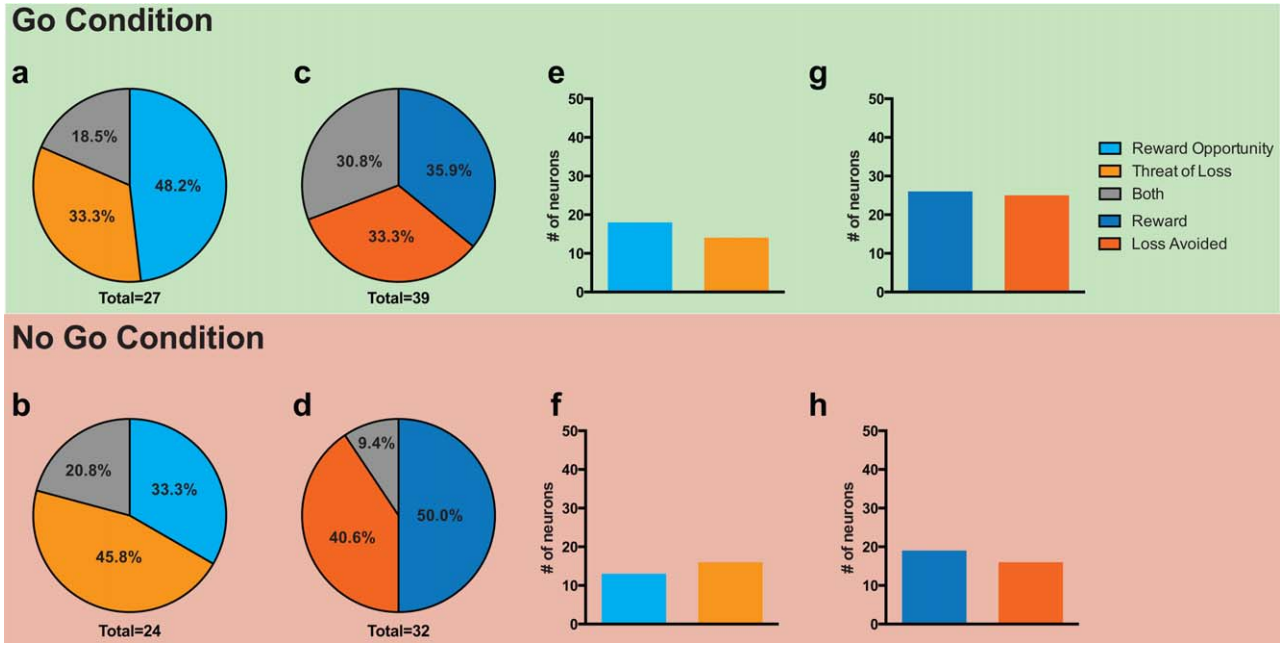

Figure 4.

GPi responsiveness to valence in stimulus and feedback conditions. Proportions of the neuronal population responding in the poststimulus period to reward opportunity, threat of loss, and both conditions during Go trials (**a**) and No Go trials (**b**). Proportions of the neuronal population responding in the post-feedback period to reward, loss avoidance, and both conditions during Go trials (**c**) and No Go trials (**d**). [reward receipt (dark blue), loss avoidance (dark orange), and both (gray)]. Total number = total number of responding neurons out of 100 neurons analyzed. Comparison of neurons responding to reward opportunity and neurons responding to threat of loss for the Go (**e**) and No Go (**f**) conditions. Comparison of neurons responding to reward obtained and loss avoided for the Go (**g**) and No Go (**h**) conditions. (*= $P < 0.05$, χ^2-test).

sagittal plane, 2.08 ± 2.55 mm posterior to the intercommissural point and 1.06 ± 1.94 mm below the AC–PC plane (Fig. 6A–C). The mean position of neuronal populations responsive to various valence stimuli are shown in Figure 6. These were well within the accepted bounds of the somatosensory GPi [DeLong et al., 1985].

DISCUSSION

Our results reveal that STN and GPi neurons in human PD patients encode multiple valence conditions, including the opportunity for reward, the threat of loss, reward receipt, and the successful avoidance of loss. Most of the responsive neurons were exclusive for specific conditions.

This is the first study to record the responses of human STN neurons to stimuli indicating an opportunity for reward or a threat of loss in both action and inhibition contexts. We show that distinct neuronal populations responded for each motivational context. In accordance with the findings of previous animal studies [Breysse et al., 2015; Lardeux et al., 2009, 2013], STN neurons were mostly specific to one of the two optimal outcomes, based on the responses observed at both stimulus presentation and feedback delivery. There was a clear tendency for STN neurons to encode the positively valenced optimal outcome (reward) versus the neutrally valenced optimal outcome (loss avoidance). Interestingly, the population responding to reward opportunity was larger than that responding to threat of loss. This suggests that the STN more strongly encoded the rewarding outcome. This finding is in line with a previous study demonstrating preferential encoding in the rat STN [Lardeux et al., 2013].

Our results corroborate the findings of previous studies that the GPi participates in reward signaling [Hong and Hikosaka, 2013; Matsumoto and Hikosaka, 2007]. Specifically, GPi neurons responded to both the expectation of reward and reward receipt. Importantly, GPi neurons also encoded the threat of loss (stimulus) and loss avoidance (feedback), suggesting that valence encoding by the GPi is not limited purely to reward.

Since the STN and GPi are well known to be involved in motor behavior, it may be argued that responses at stimulus presentation might not be strictly valence-related [Breysse et al., 2015]. Our experimental design, which held motor behavior constant while valence was modified, and which was conducted in both movement and nonmovement scenarios, should in theory permit dissociation between valence-related and motor-related activity.

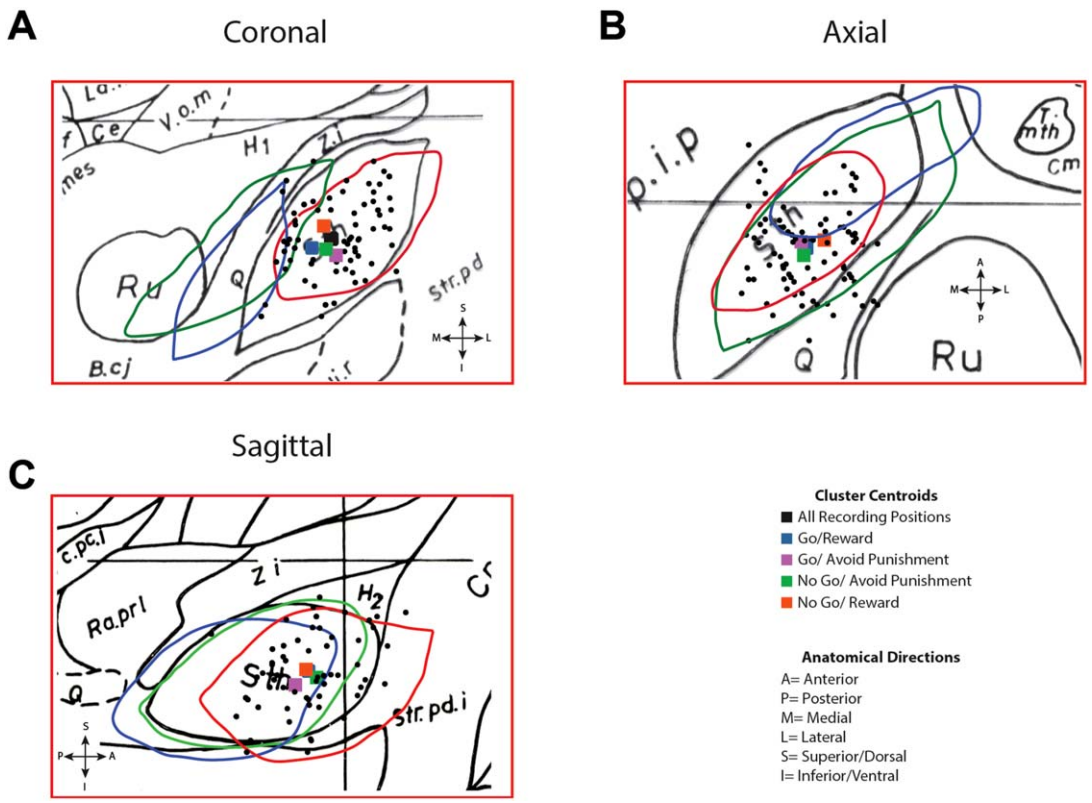

Figure 5.

Positions of Recorded STN Neurons. The spatial location of the microelectrode recording sites in STN as transposed onto the Schaltenbrand–Bailey atlas. (**a**) The STN from coronal slices F.p 4.0 (drawn in red), F.p 1.5 (drawn in green), and F.a 2.0 (drawn in blue) are superimposed on F.p 3.0 (drawn in black). (**b**) The STN from axial slices H.v −1.5, (drawn in red) H.v −3.5, (drawn in green), and H.v −6.0 (drawn in blue) are superimposed on H.v −4.5 (drawn in black). The portion of each slice shown is 10 mm by 15 mm. Black dots represent recording positions. (**c**) The STN from sagittal slices S.l 10 (drawn in red), S.l 13.5 (drawn in green), and S.l 15 (drawn in blue) are superimposed on S.l 11 (in black). Colored squares represent the centroid of clusters of neurons responsive to feedback in each of the conditions.

Experimental designs that implement a gating approach to motor response, that is, intervals between stimulus presentation and the time when a successful motor response can be registered, may permit a clearer dissociation between valence and motor activity, but they introduce an artificial component into the evaluation of action control and may obscure the character and temporal dynamics of action-valence interactions in the natural state. In addition, the possibility of overlap between movement- and valence-related activity in the feedback epoch is greatly diminished by the delay period between completion of action selection (button press or expiration of the decision interval) and feedback delivery.

The prevailing view of the functional topography of the STN is division into three zones: an anteromedial limbic zone, a posterior sensorimotor zone, and an overlapping associative zone located between the two [Joel and Weiner, 1997; Karachi et al., 2005; Lambert et al., 2012, 2015]. However, this view has recently been called into question, and a more nuanced theory has emerged suggesting a graduated change in functional topography rather than sharp anatomical boundaries [Alkemade and Forstmann, 2014; Lambert et al., 2015].

In the present study, limbic responsive neurons were not confined to the anteromedial portion of the STN, the region widely held to be the zone of limbic involvement. Still, we were unable to confirm the emergent hypothesis of a subtle functional transition across the STN's anterior and medial axes. Rather, we found that limbic processing neurons were distributed throughout the STN. It is important to note that our study was unable to sample a significant number of neurons in the anteromedial STN, due to the inherent limitations of recording neurons encountered exclusively along pre-defined trajectories for therapeutic DBS lead placement. Thus, our findings do not preclude the possibility that the anteromedial portion of the STN is more heavily involved in limbic processing (either by proportion of sampled neurons or magnitude of modulation).

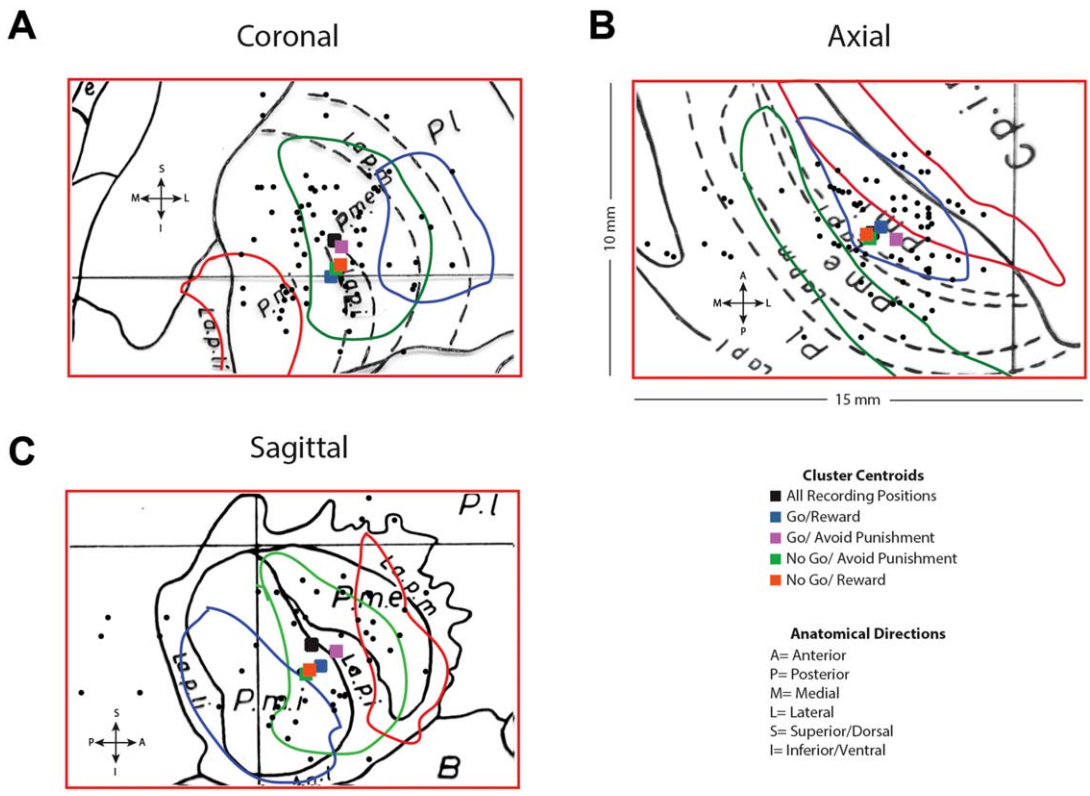

Figure 6.

Positions of Recorded GPi Neurons. The spatial location of the microelectrode recording sites in GPi as transposed onto the Schaltenbrand–Bailey atlas. (**a**) The GPi from coronal slices F.a 7.5 (drawn in red), F.a 3.0 (drawn in green), and F.a 2.0 (drawn in blue) are superimposed on F.p 5.0 (drawn in black). (**b**) The GPi from axial slices H.v −1.5 (drawn in red), H.v −3.5 (drawn in green), and H.v −6.0 (drawn in blue) are superimposed on H.v −4.5 (drawn in black). (**c**) The GPi from sagittal slices S.l 16 (drawn in red), S.l 18.5 (drawn in green), and S.l 21.5 (drawn in blue) are superimposed on S.l 20 (drawn in black). The portion of each slice shown is 10 mm by 15 mm. Black dots represent recording positions. Colored squares represent the centroid of clusters of neurons responsive to feedback in each of the conditions.

However, our results do suggest that limbic overlap with the sensorimotor region is greater than has been previously reported.

It is widely believed that limbic processing neurons in the GPi reside in the anterior portion of the nucleus. This view has been supported by limited clinical evidence suggesting enhanced limbic effects following stimulation in the anterior GPi [Cif et al., 2007; Nair et al., 2014], and immunohistochemical studies showing the anterior GPi is a recipient of limbic afferents (although, importantly, the boundaries between putative limbic and motor territories were not sharp and had significant overlap).[Karachi et al., 2002] The present study documents neurons that were responsive to valence well outside the anterior region, suggesting that limbic processing neurons may in fact be more widely distributed in the GPi than has been acknowledged elsewhere. Here again, we note that our results do not preclude a higher concentration of valence-responsive neurons in anterior GPi given that predefined electrode trajectories did not permit significant sampling from this region.

Part of the motivation to map valence-responsive neurons in these structures is to explain the occurrence of cognitive and behavioral decline following DBS utilizing either target but with the susceptibility to decline apparently greater following STN DBS [Fukaya and Yamamoto, 2015; Hershey et al., 2004; Videnovic and Metman, 2008; Witt et al., 2004, 2008; Zahodne et al., 2009; Zangaglia et al., 2009]. In this regard, we note key anatomical differences between the two structures. The human STN is approximately 140 cubic mm [During et al., 2001] and consists of approximately 250,000 neurons [Lévesque and Parent, 2005], while the human GPi is approximately 460 cubic mm [Tarsy et al., 2008] and the pallidum comprises approximately 700,000 neurons [Purves et al., 2001]. In light of (1) this size and neuronal density difference, (2)

the apparently wide distribution of valence-responsive neurons in both structures, and (3) the higher concentration of valence-responsive neurons in the STN, one plausible explanation for clinical differences in DBS targets is that the effective DBS electrical field targeting STN would incorporate more valence-responsive neurons than would a comparable electrical field targeting the GPi.

In conclusion, we report here that STN and GPi neurons encode valence-related information during action control, with valence-responsive neurons comprising a greater proportion of neurons in the STN compared to the anatomically larger GPi. Valence-responsive STN and GPi neurons appear to be evenly distributed throughout both structures. In the STN, reward-related stimuli mobilize a greater proportion of neurons than loss-related stimuli. In contrast, in the GPi, reward- and loss-related stimuli mobilize equivalent proportions of neurons. These attributes of the STN and GPi suggest that both structures occupy critical positions in decision-making circuitry, and this information may assist in explaining the numerous behavioral complications that have been associated with chronic high-frequency electrical stimulation of these structures, as well as the higher incidence of these complications following manipulation of the anatomically more compact STN. Future work elaborating on valence processing and action-valence interactions in STN and GPi in broader contexts will be important to the refinement of DBS surgery techniques and the further development of neuromodulatory therapies targeted at psychiatric disorders.

ACKNOWLEDGMENTS

MSO serves as a consultant for the National Parkinson Foundation, and has received research grants from NIH, NPF, the Michael J. Fox Foundation, the Parkinson Alliance, Smallwood Foundation, the Bachmann-Strauss Foundation, the Tourette Syndrome Association, and the UF Foundation; he has previously received honoraria, but in the past >60 months has received no support from industry. MSO has received royalties for publications with Demos, Manson, Amazon, Smashwords, Books4Patients, and Cambridge (movement disorders books); he is an associate editor for New England Journal of Medicine Journal Watch Neurology. MSO has participated in CME and educational activities on movement disorders (in the last 36) months sponsored by PeerView, Prime, QuantiaMD, WebMD, MedNet, Henry Stewart, and by Vanderbilt University. The institution and not MSO receives grants from Medtronic, Abbvie, Allergan, and ANS/St. Jude, and the PI has no financial interest in these grants. MSO participated as a site PI and/or co-I for several NIH, foundation, and industry sponsored trials over the years but has not received honoraria. PJR, OC, CP, and AG have no conflicts of interest to report. No funding sources contributed to this study.

REFERENCES

Alkemade A, Forstmann BU (2014): Do we need to revise the tripartite subdivision hypothesis of the human subthalamic nucleus (STN)? NeuroImage 95:326–329.

Bejjani BP, Dormont D, Pidoux B, Yelnik J, Damier P, Arnulf I, Bonnet AM, Marsault C, Agid Y, Philippon J, Cornu P (2000): Bilateral subthalamic stimulation for Parkinson's disease by using three-dimensional stereotactic magnetic resonance imaging and electrophysiological guidance. J Neurosurg 92:615–625.

Bischoff-Grethe A, Buxton RB, Paulus MP, Fleisher AS, Yang TT, Brown GG (2015): Striatal and pallidal activation during reward modulated movement using a translational paradigm. J Int Neuropsychol Soc 21:399–411.

Breysse E, Pelloux Y, Baunez C (2015): The good and bad differentially encoded within the subthalamic nucleus in rats,. eNeuro 2. http://www.ncbi.nlm.nih.gov/pmc/articles/PMC4607759/.

Cif L, Biolsi B, Gavarini S, Saux A, Robles SG, Tancu C, Vasques X, Coubes P (2007): Antero-ventral internal pallidum stimulation improves behavioral disorders in Lesch–Nyhan disease. Mov Disord 22:2126–2129.

Daniel SE, Lees AJ (1993): Parkinson's Disease Society Brain Bank, London: Overview and research. J Neural Transm Suppl 39: 165–172.

Darbaky Y, Baunez C, Arecchi P, Legallet E, Apicella P (2005): Reward-related neuronal activity in the subthalamic nucleus of the monkey. Neuroreport 16:1241–1244.

DeLong MR, Crutcher MD, Georgopoulos AP (1985): Primate globus pallidus and subthalamic nucleus: Functional organization. J Neurophysiol 53:530–543.

During MJ, Kaplitt MG, Stern MB, Eidelberg D (2001): Subthalamic GAD gene transfer in Parkinson disease patients who are candidates for deep brain stimulation. Hum Gene Ther 12: 1589–1591.

Espinosa-Parrilla J-F, Baunez C, Apicella P (2013): Linking reward processing to behavioral output: Motor and motivational integration in the primate subthalamic nucleus. Front Comput Neurosci 7:175.

Espinosa-Parrilla J-F, Baunez C, Apicella P (2015): Modulation of neuronal activity by reward identity in the monkey subthalamic nucleus. Eur J Neurosci 42:1705–1717.

Fukaya C, Yamamoto T (2015): Deep brain stimulation for Parkinson's disease: Recent trends and future direction. Neurol Med Chir (Tokyo) 55:422–431.

Gdowski MJ, Miller LE, Bastianen CA, Nenonene EK, Houk JC (2007): Signaling patterns of globus pallidus internal segment neurons during forearm rotation. Brain Res 1155:56–69.

Guitart-Masip M, Chowdhury R, Sharot T, Dayan P, Duzel E, Dolan RJ (2012a): Action controls dopaminergic enhancement of reward representations. Proc Natl Acad Sci USA 109: 7511–7516.

Guitart-Masip M, Huys QJM, Fuentemilla L, Dayan P, Duzel E, Dolan RJ (2012b): Go and no-go learning in reward and punishment: Interactions between affect and effect. NeuroImage 62:154–166.

Hershey T, Revilla FJ, Wernle A, Gibson PS, Dowling JL, Perlmutter JS (2004): Stimulation of STN impairs aspects of cognitive control in PD. Neurology 62:1110–1114.

Hikosaka O, Bromberg-Martin E, Hong S, Matsumoto M (2008): New insights on the subcortical representation of reward. Curr Opin Neurobiol 18:203–208.

Hong S, Hikosaka O (2013): Diverse sources of reward value signals in the basal ganglia nuclei transmitted to the lateral habenula in the monkey. Front Hum Neurosci 7:778.

Howell NA, Prescott IA, Lozano AM, Hodaie M, Voon V, Hutchison WD (2016): Preliminary evidence for human globus pallidus pars interna neurons signaling reward and sensory stimuli. Neuroscience 328:30–39.

Hutchison WD, Allan RJ, Opitz H, Levy R, Dostrovsky JO, Lang AE, Lozano AM (1998): Neurophysiological identification of the subthalamic nucleus in surgery for Parkinson's disease. Ann Neurol 44:622–628.

Joel D, Weiner I (1997): The connections of the primate subthalamic nucleus: Indirect pathways and the open-interconnected scheme of basal ganglia-thalamocortical circuitry. Brain Res Brain Res Rev 23:62–78.

Karachi C, François C, Parain K, Bardinet E, Tandé D, Hirsch E, Yelnik J (2002): Three-dimensional cartography of functional territories in the human striatopallidal complex by using calbindin immunoreactivity. J Comp Neurol 450:122–134.

Karachi C, Yelnik J, Tandé D, Tremblay L, Hirsch EC, François C (2005): The pallidosubthalamic projection: An anatomical substrate for nonmotor functions of the subthalamic nucleus in primates. Mov Disord 20:172–180.

Lambert C, Zrinzo L, Nagy Z, Lutti A, Hariz M, Foltynie T, Draganski B, Ashburner J, Frackowiak R (2012): Confirmation of functional zones within the human subthalamic nucleus: Patterns of connectivity and sub-parcellation using diffusion weighted imaging. Neuroimage 60:83–94.

Lambert C, Zrinzo L, Nagy Z, Lutti A, Hariz M, Foltynie T, Draganski B, Ashburner J, Frackowiak R (2015): Do we need to revise the tripartite subdivision hypothesis of the human subthalamic nucleus (STN)? Response to Alkemade and Forstmann. NeuroImage 110:1–2.

Lane RD, Chua PM, Dolan RJ (1999): Common effects of emotional valence, arousal and attention on neural activation during visual processing of pictures. Neuropsychologia 37:989–997.

Lardeux S, Pernaud R, Paleressompoulle D, Baunez C (2009): Beyond the reward pathway: Coding reward magnitude and error in the rat subthalamic nucleus. J Neurophysiol 102: 2526–2537.

Lardeux S, Paleressompoulle D, Pernaud R, Cador M, Baunez C (2013): Different populations of subthalamic neurons encode cocaine vs. sucrose reward and predict future error. J Neurophysiol 110:1497–1510.

Lee JI, Metman LV, Ohara S, Dougherty PM, Kim JH, Lenz FA (2007): Internal pallidal neuronal activity during mild drug-related dyskinesias in parkinson's disease: Decreased firing rates and altered firing patterns. J Neurophysiol 97:2627–2641.

Lévesque J-C, Parent A (2005): GABAergic interneurons in human subthalamic nucleus. Mov Disord 20:574–584.

Levy R, Dostrovsky JO, Lang AE, Sime E, Hutchison WD, Lozano AM (2001): Effects of apomorphine on subthalamic nucleus and globus pallidus internus neurons in patients with Parkinson's disease. J Neurophysiol 86:249–260.

Matsumoto M, Hikosaka O (2007): Lateral habenula as a source of negative reward signals in dopamine neurons. Nature 447: 1111–1115.

Nair G, Evans A, Bear RE, Velakoulis D, Bittar RG (2014): The anteromedial GPi as a new target for deep brain stimulation in obsessive compulsive disorder. J Clin Neurosci 21:815–821.

Plaha P, Ben-Shlomo Y, Patel NK, Gill SS (2006): Stimulation of the caudal zona incerta is superior to stimulation of the subthalamic nucleus in improving contralateral parkinsonism. Brain 129:1732–1747.

Purves D, Augustine GJ, Fitzpatrick D, Katz LC, LaMantia A-S, McNamara JO, Williams SM (2001): Projections from the Basal Ganglia to Other Brain Regions. Avaliable at: http://www.ncbi.nlm.nih.gov/books/NBK10860/

Rossi PJ, Gunduz A, Okun MS (2015): The subthalamic nucleus, limbic function, and impulse control. Neuropsychol Rev 25: 398–410.

Sarma SV, Cheng ML, Eden U, Williams Z, Brown EN, Eskandar E (2012): The effects of cues on neurons in the basal ganglia in Parkinson's disease. Front Integr Neurosci 6:40.

Schalk G, McFarland DJ, Hinterberger T, Birbaumer N, Wolpaw JR (2004): BCI2000: A general-purpose brain-computer interface (BCI) system. IEEE Trans Biomed Eng 51:1034–1043.

Schaltenbrand G, Bailey P (1959): Introduction to Stereotaxis with an Atlas of the Human Brain, Vol. III. Stuttgart: Georg Thieme Verlag.

Schroll H, Horn A, Gröschel C, Brücke C, Lütjens G, Schneider G-H, Krauss JK, Kühn AA, Hamker FH (2015): Differential contributions of the globus pallidus and ventral thalamus to stimulus-response learning in humans. NeuroImage 122: 233–245.

Sterio D, Zonenshayn M, Mogilner AY, Rezai AR, Kiprovski K, Kelly PJ, Beric A (2002): Neurophysiological refinement of subthalamic nucleus targeting. Neurosurgery 50:58–67, discussion 67–69.

Sudhyadhom A, Okun MS, Foote KD, Rahman M, Bova FJ (2012): A three-dimensional deformable brain atlas for DBS targeting. I. Methodology for atlas creation and artifact reduction. Open Neuroimaging J 6:92–98.

Tarsy D, Vitek JL, Starr P, Okun M (2008): Deep Brain Stimulation in Neurological and Psychiatric Disorders. Springer Science & Business Media.

Teagarden MA, Rebec GV (2007): Subthalamic and striatal neurons concurrently process motor, limbic, and associative information in rats performing an operant task. J Neurophysiol 97: 2042–2058.

Toleikis JR, Metman LV, Pilitsis JG, Barborica A, Toleikis SC, Bakay RAE (2012): Effect of intraoperative subthalamic nucleus DBS on human single-unit activity in the ipsilateral and contralateral subthalamic nucleus. J Neurosurg 116: 1134–1143.

Videnovic A, Metman LV (2008): Deep brain stimulation for Parkinson's disease: Prevalence of adverse events and need for standardized reporting. Mov Disord 23:343–349.

Witjas T, Baunez C, Henry JM, Delfini M, Regis J, Cherif AA, Peragut JC, Azulay JP (2005): Addiction in Parkinson's disease: Impact of subthalamic nucleus deep brain stimulation. Mov Disord 20:1052–1055.

Witt K, Pulkowski U, Herzog J, Lorenz D, Hamel W, Deuschl G, Krack P (2004): Deep brain stimulation of the subthalamic nucleus improves cognitive flexibility but impairs response inhibition in Parkinson disease. Arch Neurol 61:697–700.

Witt K, Daniels C, Reiff J, Krack P, Volkmann J, Pinsker MO, Krause M, Tronnier V, Kloss M, Schnitzler A, Wojtecki L, Bötzel K, Danek A, Hilker R, Sturm V, Kupsch A, Karner E, Deuschl G (2008): Neuropsychological and psychiatric changes after deep brain stimulation for Parkinson's disease: A randomised, multicentre study. Lancet Neurol 7:605–614.

van Wouwe NC, van den Wildenberg WPM, Ridderinkhof KR, Claassen DO, Neimat JS, Wylie SA (2015): Easy to learn, hard

to suppress: The impact of learned stimulus–outcome associations on subsequent action control. Brain Cogn 101:17–34.

Zahodne LB, Okun MS, Foote KD, Fernandez HH, Rodriguez RL, Wu SS, Kirsch-Darrow L, Jacobson CE, Rosado C, Bowers D (2009): Greater improvement in quality of life following unilateral deep brain stimulation surgery in the globus pallidus as compared to the subthalamic nucleus. J Neurol 256: 1321–1329.

Zangaglia R, Pacchetti C, Pasotti C, Mancini F, Servello D, Sinforiani E, Cristina S, Sassi M, Nappi G (2009): Deep brain stimulation and cognitive functions in Parkinson's disease: A three-year controlled study. Mov Disord 24:1621–1628.

Zimnik AJ, Nora GJ, Desmurget M, Turner RS (2015): Movement-related discharge in the macaque globus pallidus during high-frequency stimulation of the subthalamic nucleus. J Neurosci 35:3978–3989.